Resistance of Omicron subvariants BA.2.75.2, BA.4.6 and BQ.1.1 to neutralizing antibodies

Delphine Planas[1,2,#], Timothée Bruel[1,2], Isabelle Staropoli[1], Florence Guivel-Benhassine[1], Françoise Porrot[1], Piet Maes[3], Ludivine Grzelak[1], Matthieu Prot[4], Said Mougari[4], Cyril Planchais[5], Julien Puech[6], Madelina Saliba[6], Riwan Sahraoui[6], Florent Fémy[7], Nathalie Morel[8], Jérémy Dufloo[9], Rafael Sanjuán[9,10], Hugo Mouquet[5], Emmanuel André[11,12], Laurent Hocqueloux[13], Etienne Simon-Loriere[4], David Veyer[6,14], Thierry Prazuck [13*], Hélène Péré[6,14**] & Olivier Schwartz[1,2#*]

[1]Virus and Immunity Unit, Institut Pasteur, Université Paris Cité, CNRS UMR3569, Paris, France.
[2]Vaccine Research Institute, Créteil, France.
[3]KU Leuven, Department of Microbiology, Immunology and Transplantation, Laboratory of Clinical and Epidemiological Virology, Leuven, Belgium.
[4]G5 Evolutionary Genomics of RNA Viruses, Institut Pasteur, Université Paris Cité, Paris, France.
[5]Humoral Immunology Laboratory, Institut Pasteur, Université Paris Cité, INSERM U1222, Paris, France.
[6]Laboratoire de Virologie, Service de Microbiologie, Hôpital Européen Georges Pompidou, Paris, France.
[7]Service d'accueil des urgences, Hôpital Européen Georges Pompidou, Paris, France.
[8]Service de Pharmacologie et Immunoanalyse (SPI), CEA, INRA, Université Paris-Saclay, F-91191 Gif-sur Yvette, France
[9]Institute for Integrative Systems Biology (I2SysBio), Universitat de València-CSIC, 46980 Paterna, València,
[10]Department of Genetics, Universitat de València, València, Spain.
[11]University Hospitals Leuven, Department of Laboratory Medicine, National Reference Centre for Respiratory Pathogens, Leuven, Belgium.
[12]KU Leuven, Department of Microbiology, Immunology and Transplantation, Laboratory of Clinical Microbiology, Leuven, Belgium.
[13]CHR d'Orléans, Service de Maladies Infectieuses, Orléans, France.
[14]Functional Genomics of Solid Tumors (FunGeST), Centre de Recherche des Cordeliers, INSERM, Université de Paris, Sorbonne Université, Paris, France.

[#]Correspondence to delphine.planas@pasteur.fr and olivier.schwartz@pasteur.fr
*Co-last authors

Abstract

Convergent evolution of SARS-CoV-2 Omicron BA.2, BA.4 and BA.5 lineages has led to the emergence of several new subvariants, including BA.2.75.2, BA.4.6. and BQ.1.1. The subvariants BA.2.75.2 and BQ.1.1 are expected to become predominant in many countries in November 2022. They carry an additional and often redundant set of mutations in the spike, likely responsible for increased transmissibility and immune evasion. Here, we established a viral amplification procedure to easily isolate Omicron strains. We examined their sensitivity to 6 therapeutic monoclonal antibodies (mAbs) and to 72 sera from Pfizer BNT162b2-vaccinated individuals, with or without BA.1/BA.2 or BA.5 breakthrough infection. Ronapreve (Casirivimab and Imdevimab) and Evusheld (Cilgavimab and Tixagevimab) lost any antiviral efficacy against BA.2.75.2 and BQ.1.1, whereas Xevudy (Sotrovimab) remained weakly active. BQ.1.1 was also resistant to Bebtelovimab. Neutralizing titers in triply vaccinated individuals were low to undetectable against BQ.1.1 and BA.2.75.2, 4 months after boosting. A BA.1/BA.2 breakthrough infection increased these titers, which remained about 18-fold lower against BA.2.75.2 and BQ.1.1, than against BA.1. Reciprocally, a BA.5 breakthrough infection increased more efficiently neutralization against BA.5 and BQ.1.1 than against BA.2.75.2. Thus, the evolution trajectory of novel Omicron subvariants facilitated their spread in immunized populations and raises concerns about the efficacy of most currently available mAbs.

Introduction

Successive sub-lineages of Omicron have spread worldwide since the identification of BA.1 in November 2021 [1,2]. Probably more than 80% of the population were infected by one or another Omicron subvariant in less than one year [3] [4], without efficient protection against infection conferred by vaccination [5] [6] [7]. The incidence of breakthrough infections in vaccinated individuals has thus increased with Omicron [8] [3]. All Omicron lineages exbibit considerable immune evasion properties. BA.1 and BA.2 contained about 32 changes in the spike protein, promoting immune escape and high transmissibility [9] [10] [11]. BA.5 was then predominant in many countries by mid-2022 and was responsible for a novel peak of contaminations [2] [12]. BA.4 and BA.5 bear the same spike, with 4 additional modifications when compared to BA.2. The neutralizing activity of sera from COVID-19 vaccine recipients was further reduced against BA.4/BA.5 by about 3-5 fold compared to BA.1 and BA.2 [13,14] [15] [16]. Novel sub-variants with enhanced transmissibility rates, derived from either BA.2 or BA.4/BA.5, rapidly emerged and should become prevalent in November 2022. Their geographical distribution is heterogeneous, but they carry an additional limited set of mutations in the spike. For instance, BA.2.75.2, derived from BA.2, was first noted in India and Singapore and comprises R346T, F486S and D1199N substitutions [17-19]. BA.4.6 was detected in various countries, including USA and UK, and carries R346T and N658S mutations [20] [21]. As of November 2022, BQ.1.1 became the main circulating lineage in many countries. It also carries the R346T mutation found in BA.2.75.2, along with K444T and N460K substitutions [22]. The R346T mutation has been associated with escape from monoclonal antibodies (mAbs) and from vaccine-induced antibodies [19] [18] [23]. This convergent evolution of the spike suggests that the different circulating SARS-CoV-2 sub-lineages faced a similar selective pressure, probably exerted by preexisting or imprinted immunity [23] [24]. A characterization of these new viruses is needed to evaluate their potential impact.

A few recent articles and preprints reported an extensive escape of these Omicron subvariants to neutralization, studying sera from individuals who received three or four vaccine doses, including a bivalent booster [25] [26] [17,27]. Most of these studies were performed with lentiviral or VSV pseudotypes. In one preprint [17], recombinant SARS-CoV-2 viruses carrying spikes from Omicron sublineages in an ancestral SARS-CoV-2 backbone were generated, but they might behave somewhat differently than authentic isolates.

Here, we identified and used a highly permissive cell line to amplify BA.2.75.2, BA.4.6. and BQ.1.1 isolates. We analyzed the sensitivity of these strains to approved mAbs, to sera from Pfizer BNT162b2 vaccine recipients, and to individuals with BA.1/BA.2 or BA.5 breakthrough infections.

Results

Rapid isolation of Omicron subvariants with the IGROV-1 cell line.

SARS-CoV-2 strains are classically isolated and amplified in Vero E6 or Vero-TMPRSS2+ cells. Vero cells are african green monkey kidney epithelial cells that were derived in the 1960s. They are defective in type-I interferon production and sensitive to many viral species [28]. However, upon serial passages in Vero E6 cells, SARS-CoV-2 may acquire adaptive spike mutations, with modification or deletion of the furin-like cleavage site, resulting in phenotypic changes in plaque assays [29]. Omicron isolates are growing less efficiently in Vero E6 and Vero-TMPRSS2+ cells than previous SARS-CoV-2 variants, probably because Omicron relies more on endocytic proteases and less on TMPRSS2 than other variants [30,31]. This may explain why infectious viral loads measured in nasopharyngeal swabs from Omicron-infected individuals appeared lower than those infected with Delta, despite an enhanced transmissibility of Omicron [32]. We thus sought another cell line that may be more adapted to isolation and replication of Omicron subvariants than Vero cells. To this aim, we screened a panel of cells and observed that IGROV-1 cells were highly permissive to Omicron. IGROV-1 cells originated from an ovarian carcinoma and were established in 1985 [33]. IGROV-1 cells naturally express low levels of ACE2 and TMPRSS2, as assessed by flow cytometry (Extended data Fig. 1).

We compared the permissibility of Vero-TMPRSS2+ and IGROV-1 cells to Omicron and Delta. We titrated infectious viral loads in nasopharyngeal swabs from 53 Delta and 81 Omicron (BA.1) infected individuals collected at the Hôpital Européen Georges Pompidou (HEGP) in Paris. The characteristics of the patients (age, sex, days post onset of symptoms, vaccination status) appear in Supplementary Table 1. Nasopharyngeal swabs were serially diluted and incubated with either Vero-TMPRSS2+ or IGROV-1 cells. After 48h, cells were stained with an anti-SARS-CoV-2 N monoclonal antibody. Foci of infected cells were scored with an automated confocal microscope. A representative experiment with Delta and Omicron positive samples demonstrated a high sensitivity of IGROV-1 to Omicron (Extended data Fig. 2).

The 134 samples were ranked according to their viral RNA levels measured by RT-qPCR, from low to high Ct (Fig. 1a). With Delta-positive samples, there was no major difference in infectious viral titers calculated with Vero-TMPRSS2+ or IGROV-1 cells which inversely correlated with Ct (Fig. 1b,c). We did not detect infectious virus in samples with Ct>27. About 35% of Delta positive samples carried infectious virus (Fig 1d,e). The situation was different with Omicron BA.1 positive samples. We did not detect Omicron-infected Vero-TMPRSS2+ cells, even in samples with low Ct, at this early time-point (48h). In contrast, 52% of the samples from Omicron-infected individuals were positive when titrated on IGROV-1 cells (Fig. 1c,d,e), confirming that these cells are particularly sensitive to Omicron BA.1.

We next isolated BA.4.6 and BQ.1.1 variants from nasopharyngeal swabs collected at HEGP using IGROV-1 cells. As with BA.1, numerous foci of infected cells were detected at 2 days post-infection

(p.i.) and supernatants were harvested at days 2 or 3 p.i., yelding high titers with the S-Fuse reporter cells. S-Fuse cells form syncytia and become GFP+ upon infection, allowing overnight measurement of viral infectivity and neutralizing antibody activity [34,35]. Sequences of the variants after one passage on IGROV-1 cells identified BA.4.6 and BQ.1.1 (Pango lineage B.1.1.529.4.6 and B.1.1.529.5.3.1.1.1.1.1.1, respectively according to Nextstrain, GISAID accession ID: BA.4.6: EPI_ISL_15729633 and BQ.1.1: EPI_ISL_15731523), indicating that no adaptative mutations were generated during this short culture period. As expected, BA.4.6 included R346T and N658S mutations [20][21] and BQ.1.1 carried R346T, K444T and N460K substitutions [22]. The spike mutations in the main Omicron subvariants are depicted Fig. 2.

We also isolated a BA.2.75.2 variant from a nasopharyngeal swab from the National Reference Center of UZ/KU Leuven (Belgium). The virus was initially amplified by two passages on Vero E6 cells, but the resulting viral titers were low. We thus performed one supplementary passage on IGROV-1 cells, which significantly increased the titers to $4x10^5$ pfu/ml in 48 hours. Sequencing of the virus confirmed the presence of BA.2.75.2 (Pango lineage B.1.1.529.2.75.2, according to Nextstrain, GISAID accession ID: E EPI_ISL_15731524). When compared to BA.2.75, the BA.2.75.2 spike protein contained 3 additional mutations, R346T and F486S in the RBD, and D1199N in the HR2 (Heptad Repeat 2) region, located in the S2 domain and involved in fusion (Fig. 2).

Syncytia were observed in BA.2.75.2, BA.4.6. and BQ.1.1-infected S-Fuse cells (Extended Data Fig. 3). The three variants generated syncytia of similar size, that were smaller than those formed by the ancestral D614G strain (Extended Data Fig. 3). It will be worth further examining whether other Omicron subvariants may display different fusogenic potential in different cell types.

Altogether, these results show that IGROV-1 cells are highly sensitive to Omicron. They allow a rapid titration of infectivity present in nasopharyngeal swabs from infected individuals, as well as a one-passage amplification of Omicron subvariants. Future work will help determining the underlying cellular mechanisms and whether entry or other steps of the viral cycle are facilitated in IGROV-1 cells.

Neutralization of BA.2.75.2, BA.4.6. and BQ.1.1 by approved monoclonal antibodies

Several anti-spike monoclonal antibodies (mAbs) are used as pre-exposure prophylaxis (PrEP) or post-exposure therapy in individuals at risk for severe disease [36]. These mAbs belong to the four main classes of anti-RBD antibodies which are defined by their binding site [36,37]. Prophylaxis based on Ronapreve (Imdevimab + Casirivimab) or Evusheld (Cilgavimab + Tixagevimab) cocktails provided about 80% protection against symptomatic infection [38,39]. Post-infection treatment with Xevudy (Sotrovimab) reached 85% efficacy in preventing COVID-19-related hospitalization or death [36,40]. However, Omicron BA.1, BA.2 and BA.5 escaped neutralization from a large part of these mAbs, leading to changes in treatment guidelines [41,42]. As of mid-2022, Ronapreve and Sotrovimab were no longer approved and a double dose of Evusheld was recommended. Bebtelovimab is another potent mAb,

similarly effective against ancestral strains and BA.1 and BA.2 [43], currently only available in United States [44].

We thus assessed with the S-Fuse assay the sensitivity of BA.2.75.2, BA.4.6. and BQ.1.1 to mAbs that are currently authorized (Cilgavimab, Tixagevimab and Bebtelovimab) or were withdrew because of Omicron escape (Sotrovimab, Casirivimab and Imdevimab). As controls, we included the ancestral D614G strain (Fig. 3a,b). Cilgavimab and Tixagevimab, alone or in combination, as well as Casirivimab, lost any neutralization activity against the three Omicron variants. Imdevinab inhibited BA.4.6 (IC50 220 ng/ml) but was inactive against BA.2.75.2 and BQ.1.1. Bebtelovimab was efficient against BA.4.6 and BA.2.75.2 (IC50 2.7 and 4.3 ng/ml, respectively) but did not neutralize BQ.1.1. Sotrovimab was the only mAb active, albeit weakly, against BA.2.75.2, BA.4.6. and BQ.1.1. With Sotrovimab, the IC50s ranged from 2,874 to 19,391 ng/ml, which represents a 45-to-300-fold increase compared to D641G.

These results demonstrate that the prevalent BA.2.75.2 and BQ.1.1 strains are resistant or weakly sensitive to currently approved mAbs.

Cohort design

We collected 72 sera from a cohort of 35 health-care workers, in Orleans, France. We previously studied the ability of some of these sera to neutralize Alpha, Beta, Delta, Omicron BA.1 and BA.5 variants [11,16]. The characteristics of the participants are indicated in Supplemental Table 1. The participants, that were not previously infected at the time of inclusion, received two doses of Pfizer BNT162b2 vaccine within an interval of 21-28 days and a booster dose 164 to 314 days later. 30 out of 35 individuals experienced a pauci-symptomatic breakthrough Omicron infection 60 to 359 days after the third injection. Screening by PCR or whole viral genome sequencing identified the Omicron subvariant responsible for the breakthrough infection. A first group of 16 individuals was infected between December 2021 and mid-June 2022, a period when BA.1 and BA.2 were successively dominant in France [45]. A second group of 15 individuals was infected between July and October 2022 and was positive BA.5. The days of vaccination, breakthrough infection and sampling are displayed in Supplemental Table 2.

Sensitivity of BA.2.75.2, BA.4.6. and BQ.1.1 to sera from vaccinees.

We asked whether vaccine-elicited antibodies neutralized the novel Omicron subvariants. Eighteen individuals were analyzed early (1 month post third dose) and ten individuals at a later time-point (4 months post third dose). We measured the potency of their sera against BA.2.75.2, BA.4.6. and BQ.1.1. We used as controls the D614G ancestral strain (belonging to the basal B.1 lineage), as well as BA.1 and BA.5 (Fig. 4a). We calculated the ED50 (Effective Dose 50%) for each combination of serum and virus. One month after the booster dose, ED50 were high for D614G (ED50 of 5×10^3) and

were decreased by 8- and 15-fold for BA.1 (ED50 of 7×10^2) and BA.5 (ED50 of 3×10^2) respectively, confirming the antibody escape properties of these previous sublineages. With BA.4.6. and BQ.1.1, the ED50 were low and within the range of those observed with the parental BA.5 strain. BA.2.75.2 neutralization titers were even lower (11-fold lower than BA.1). A similar trend was observed at a later time-point. Neutralization was reduced against all strains, highlighting the declining humoral response [11,16]. The neutralizing activity was either undetectable or barely detectable against BA.2.75.2, BA.4.6. and BQ.1.1 (Fig. 3a).

Altogether, these results indicate that the prevalent Omicron subvariants are poorly or not neutralized by vaccinees' sera sampled 4 months after a third vaccine dose.

Impact of BA.1/BA.2 breakthrough infections on neutralization of Omicron subvariants

We then examined the impact of BA.1/BA.2 breakthrough infections on the cross-neutralizing activity of serum antibodies. Eighteen individuals were analyzed at 3 months. Among them, 11 individuals were resampled 8 months after infection to evaluate the evolution of the humoral response. After 3 months, a strong augmentation of neutralization against D614G and BA.1 was observed, with ED50 above 10^4 (Fig. 4b). Compared to BA.1, the Nab titers were reduced by about 7-fold against BA.5 and BA.4.6 (ED50 of 1.5×10^3 and 1.8×10^3, respectively) and reduced by 18-fold against BA.2.75.2 and BQ.1.1 (ED50 of 6×10^2 and 7×10^2, respectively). Neutralizing titers differently declined depending on the viral isolate. Eight months after infection, titers remained high against D614G and BA.1 (ED50 of 8×10^4 and 3×10^4, respectively). The decline was stronger against BA.5 and BA.4.6 (ED50 of 4×10^2) and even more marked against BA.2.75.2 and BQ.1.1 (ED50 of 2×10^2). Therefore, post-vaccination infection by BA.1/BA.2 led to an increase in Omicron-specific neutralizing antibody titers, with disparities between variants. The anti-BA.1 response was higher than against BA.5 and BA.4.6, whereas BA.2.75.2 and BQ.1.1 were less sensitive to neutralization.

Impact of BA.5 breakthrough infections on neutralization of Omicron subvariants

The distinct neutralization profile of BA.2.75.2, BA.4.6. and BQ.1.1 after BA.1/BA.2 infection led us to examine the consequences of a BA.5 breakthrough infection on neutralization. We assessed the sera of fifteen individuals, about one month after BA.5 infection. As for BA.1/BA.2 breakthrough infection, we observed a strong augmentation of neutralization against D614G, with ED50 reaching 3×10^4 (Fig. 4c). The neutralization of BA.5 variants (BA.5 and BQ.1.1) was high (ED50 of 10^4) and somewhat lower for the BA.2-derived BA.2.75.2 strain (ED50 of 1×10^3). The neutralization activity against BA.1 was less potent after a BA.5 infection than after a BA.1/BA.2 infection (ED50 of 6×10^3 and 1×10^4, respectively) (Fig. 4b,c).

Altogether, these results indicate that a BA.5 breakthrough infection triggers a better neutralization of viral isolates of the BA.5 lineage than BA.1/BA.2-derived strains. Conversely, A BA.1/BA.2 breakthrough infection favors neutralization of BA.1 and BA.2 derived strains, relative to the BA.5 lineage.

Discussion

We report here a simple method to isolate and grow Omicron strains. We identify IGROV-1 cells as being highly permissive to Omicron, through reasons that remain to be determined. Omicron is less replicative and fusogenic than Delta in various human cell lines including Vero, Calu-3, A549-ACE2, HeLa-ACE2/TMPRSS2 and U2OS-derived S-Fuse cells [11,16,46,47]. Omicron strains inefficiently use TMPRSS2, which promotes viral entry through plasma membrane fusion, with greater dependency on endocytic entry [30,31]. Several lines of evidence indicate that the evolution of Omicron sublineages towards increased transmissibility is associated with greater fitness in human primary cells. BA.1 potently replicates in nasal epithelial cultures [30]. BA.4 and BA.5 replicate more efficiently than BA.2 in alveolar epithelial cells and are more fusogenic [48]. BA.2.75.2 growth efficiency in alveolar epithelial cells and spike-mediated fusion in Calu-3 cells are also higher than those of BA.2 [49,50]. We did not observe an enhanced cell-cell fusogenicity of BA.2.75.2, BA.4.6. and BQ.1.1 compared to BA.5, at least in S-Fuse cells, but it will be worth further examining viral fitness and fusion of these strains in IGROV-1 or primary cells.

Our results show that IGROV-1 cells recapitulate the permissibility of primary human nasal or alveolar cells to Omicron strains. Future work will help understanding viral entry pathways and replication in IGROV-1 cells. Whatever the underlying mechanisms, these cells proved useful to amplify BA.2.75.2, BA.4.6. and BQ.1.1 in a single passage, avoiding or minimizing the risk of selection of culture adaptative mutations [29]. IGROV-1 cells are also sensitive to previous SARS-CoV-2 variants. Combining viral isolation in IGROV-1 cells with the S-Fuse neutralization assay provides a rapid procedure to evaluate the properties of novel and forthcoming SARS-CoV-2 variants of concern.

We demonstrate that the currently approved or recently withdrawn therapeutic mAbs lost most of their neutralization potential against these Omicron subvariants. Evusheld no longer neutralized BA.2.75.2, BA.4.6. and BQ.1.1. Bebtelovimab was active against BA.2.75.2 and BA.4.6. but not against BQ.1.1. This fits with the observation that the K444 residue, mutated in BQ.1.1 (K444T) but not in BA.2.75.2 and BA.4.6, is important for Bebtelovimab activity [43]. Ronapreve was active against BA.4.6 but not against the prevalent BA.2.75.2 and BQ.1.1 isolates. Sotrovimab retained a relatively low neutralization activity against all strains, with IC50 ranging from 3 to more than 9 µg/ml. Sotrovimab also displays non-neutralizing antiviral activities, including ADCC [51] [52]. Sotrovimab remains clinically active against BA.2 [53]. It will be of interest determining whether Sotrovimab could maintain some

activity in vivo against these novel Omicron subvariants, despite reduced neutralization. This will help addressing the debate on the need to reassess WHO's therapeutics and COVID-19 living guideline on mAbs [54]. Overall, our results are in line with a recent preprint using lentiviral pseudotypes [23] and raise important concerns regarding the prophylactic and therapeutic administration of currently approved mAbs. Novel mAbs, with broad cross-neutralizing activities and inhibiting most of Omicron sublineages have been identified [23,55] and are warranted to extend the arsenal of mAb-based treatments.

We report that sera from individuals who had received three doses of COVID-19 Pfizer BNT162b2 vaccine displayed reduced neutralization activity against the Omicron subvariants. One month after a first booster, ED50 displayed a 10- to 80-fold decrease compared to the ancestral D614G strain. At 4 months post vaccination, neutralization was undetectable for BA.2.75.2 and slightly above background for BA.4.6. and BQ.1.1. These results suggest an abbreviated efficacy of Pfizer BNT162b2 vaccine against the three variants, extending our previous results with BA.1 and BA.5 [16]. The advantage of administrating monovalent or bivalent boosters is under scrutiny [25,27] [56] [57]. Preliminary preprints using lentiviral pseudotypes indicated that BA.5, BA.4.6 or BA.2.75 titers were comparable after monovalent or BA.5 bivalent boosters [25,27]. In contrast, when using tests based on recombinant SARS-CoV-2 infectious virus carrying spikes from different Omicron sublineages, it was observed that bivalent mRNA booster may broaden humoral immunity [26]. These discrepancies may be due to differences in experimental systems, the delay between booster administration and blood sampling and/or variation in immune imprinting across cohorts. Future work with authentic field isolates and well-characterized sera, combined with real-world vaccine efficacy data [58], will help characterizing the interest of bivalent vaccines against Omicron subvariants.

We observed a dichotomy of the neutralizing response after BA.1/BA.2 or BA.5 breakthrough infection in vaccinated individuals. In both cases, the Nabs were particularly high against D614G, highlighting the role of immune imprinting in anamnestic responses [55]. However, after BA.1/BA.2 infection, sera also potently neutralized BA.1 but there was a 6 to 18-fold reduction in efficacy against BA.2.75.2, BA.4.6. and BQ.1.1. Conversely, after BA.5 breakthrough infection, titers were higher against BA.5-derived variants than against BA.1 or BA.2.75.2. It has been reported that vaccinated individuals infected during the first Omicron wave showed enhanced immunity against earlier variants but reduced nAb potency and T cell responses against Omicron [59]. This was not exactly the case in our study, indicating that in addition to imprinted memory, responses targeting novel antigens can be generated. Besides the RBD, antibodies targeting other regions of the spike, such as the NTD or S2 region may also broaden the humoral response [60,61]. The interval between prior SARS-CoV-2 infection and booster vaccination impacts magnitude and quality of antibody and B cell responses [62]. This raises important questions regarding the frequency of booster doses, particularly in the presence of Omicron variants with greater immune evasion properties.

8

There are several limitations to our study, notably the limited number of individuals analyzed. However, the differences between strains and categories of individuals were sufficiently marked to reach statistical significance. We did not consider the effect of innate and cellular immunity on BA.2.75.2, BA.4.6. and BQ.1.1 strains. We focused our work on Pfizer vaccine recipients and did not assess the neutralization conferred by a fourth dose. We did not characterize other Omicron subvariants, such as XBB, a recombinant virus between two Omicron strains (BJ.1 and BM.1.1). Future studies will help evaluating long-term immune responses to Omicron subvariants after infection and/or vaccination.

In summary, we show here that the few convergent mutations present in the spike of BA.2 or BA.5 subvariants led to resistance to most of available therapeutic mAbs and strongly impaired the efficacy of vaccine-elicited antibodies. Breakthrough infections in triply vaccinated individuals stimulate cross-neutralizing responses with distinct efficacy depending on the variant responsible for the infection. The evolution trajectory of the novel Omicron subvariants likely reflects their continuous circulation in immunized populations.

Contributions

Experimental strategy design, experiments: D.P., T.B., I.S., F.G-B., F.P., L.G., O.S.

Vital materials: P.M., C.P., J.P., M.S., R.S., F.F., N.M., J.D., R.S., H.M., E.A., L.H., D.V., T.P., H.P.

Viral sequencing: P.M., M.P., S.M., J.P., E.S-L., D.V., H.P.

Manuscript writing and editing: D.P., T.B., O.S.

Methods

No statistical methods were used to predetermine sample size and the experiments were not randomized. The investigators were not blinded. Our research fulfills all relevant ethical requirements.

Cohorts

Serum from vaccinated and BA.1/2 and BA.5 breakthrough infected individuals (Orléans cohort). A prospective, monocentric, longitudinal, interventional cohort clinical study (ABCOVID) is conducted since 27 August 2020 with the objective to study the kinetics of COVID-19 antibodies in patients with confirmed SARS-CoV-2 infection (NCT04750720). A sub-study aimed to describe the kinetic of neutralizing antibodies after vaccination. The cohort was previously described [11,16]. This study was approved by the Ile-de-France IV ethical committee. At enrollment, written informed consent was collected and participants completed a questionnaire covering sociodemographic characteristics. Virological findings (SARS-CoV-2 RT–qPCR results, date of positive test, screening, or sequences results) and data related to SARS-CoV-2 vaccination (brand product, date of first, second, third and fourth vaccination) were also collected.

Nasopharyngeal swabs from infected individuals (Hôpital Européen Georges Pompidou). 134 nasopharyngeal swabs collected for standard care between December 2, 2021 and January 5, 2022 were retrospectively analyzed to investigate Delta and Omicron BA.1 replication. This study was carried out in accordance with the Declaration of Helsinki with no sampling addition to usual procedures and was evaluated by the ethics committee "Comité d'éthique de la recherche AP-HP Centre" affiliated to the AP-HP (Assistance publique des Hopitaux de Paris; IRB registration # 00011928). An informed consent was obtained from all participants. Swab specimens were collected for standard diagnostic following medical prescriptions in HEGP and stored at -80°C prior to infectivity measurements and viral isolations.

Virus strains and cells

The reference D614G strain (hCoV-19/France/GE1973/2020) was supplied by the National Reference Center for Respiratory Viruses hosted by Institut Pasteur and headed by S. van der Werf. This strain was obtained through the European Virus Archive goes Global (Evag) platform, a project that has received funding from the European Union's Horizon 2020 research and innovation program under grant agreement no 653316. The BA.2.75.2 strain was isolated and sequenced by the NRC UZ/KU Leuven (Leuven, Belgium). BQ.1.1 and BA.4.6 were isolated from a nasopharyngeal swab of individuals attending the emergency room of Hôpital Européen Georges Pompidou (HEGP; Assistance Publique, Hôpitaux de Paris). The swabs were sequenced by the laboratory of Virology of HEGP. All patients

provided informed consent for the use of the biological materials. The variant strains were isolated from nasopharyngeal swabs using Vero E6 or IGROV-1 cells. Viral strains were amplified by one or two passages on Vero cells. Only one passage was necessary for the amplification on IGROV-1 cells. Supernatants were harvested 2 or 3 days after viral exposure. Titration of viral stocks was performed on Vero E6 cells, with a limiting dilution technique enabling the calculation of the median tissue culture infectious dose or on S-Fuse cells. Viral supernatants were sequenced directly from the nasopharyngeal swabs, and after their isolation and amplification on Vero or IGROV-1 cells. For sequencing, we used an untargeted metagenomic sequencing approach with ribosomal RNA (rRNA) depletion. Briefly, RNA was extracted with the QIAamp Viral RNA extraction kit (Qiagen), with the poly-A RNA carrier provided. Prior to library construction, carrier RNA and host rRNA were depleted using oligo (dT) and custom probes respectively. The RNA resulting from selective depletion was used for random-primed cDNA synthesis using the SuperScript IV RT (Invitrogen). Second-strand cDNA was generated using Escherichia coli DNA ligase, RNAse H and DNA polymerase (New England Biolabs) and purified using Agencourt AMPure XP beads (Beckman Coulter). Libraries were then prepared using the Nextera XT kit and sequenced on an Illumina NextSeq500 platform (2x75 cycles). Reads were assembled using megahit v1.2.9. The sequences were deposited on GISAID (D614G: EPI_ISL_414631; BA.1 ID: EPI_ISL_6794907; BA.5 ID: EPI_ISL_13660702; BA.2.75.2 ID: EPI_ISL_15731524; BQ.1.1 ID: EPI_ISL_15731523; BA.4.6 ID: EPI_ISL_15729633). Vero E6 and Vero-TMPRSS2 were described previously [34,63]. IGROV-1 cells were obtained from Rafael Sanjuan (Universitat de València, Spain).

S-Fuse neutralization assay

U2OS-ACE2 GFP1-10 or GFP 11 cells, also termed S-Fuse cells, become GFP+ when they are productively infected by SARS-CoV-2 [34] [35]. Cells tested negative for mycoplasma. Cells were mixed (ratio 1:1) and plated at 8×10^3 per well in a µClear 96-well plate (Greiner Bio-One). The indicated SARS-CoV-2 strains were incubated with serially diluted monoclonal antibodies or sera for 15 min at room temperature and added to S-Fuse cells. Sera were heat-inactivated for 30 min at 56 °C before use. 18 h later, cells were fixed with 2% PFA, washed and stained with Hoechst (dilution of 1:1,000, Invitrogen). Images were acquired using an Opera Phenix high-content confocal microscope (PerkinElmer). The GFP area and the number of nuclei were quantified using the Harmony software (PerkinElmer). The percentage of neutralization was calculated using the number of syncytia as value with the following formula: 100 × (1 – (value with serum – value in 'non-infected')/(value in 'no serum' – value in 'non-infected')). Neutralizing activity of each serum was expressed as the half maximal effective dilution (ED50). ED50 values (in ng/ml for monoclonal antibodies and in dilution values – i.e titers – for sera) were calculated with a reconstructed curve using the percentage of neutralization at each concentration.

Nasopharyngeal swabs infectivity

Vero and IGROV-1 cells were plated at 30,000 cells per well in a mClear 96-well plate (Greiner Bio-One). The nasopharyngeal swabs were added to the Vero or IGROV-1 cells at serial dilutions from 1:10 to 1:31 250 as described previously [63]. 48 hours later, cells were fixed with 2% PFA (Electron microscopy cat# 15714-S). Cells were washed and stained intracellularly in 0.05% saponin with the anti-SARS-CoV-2 nucleoprotein (N) antibody NCP-1 for 2 hours. Cells were washed and intracellularly stained with an anti-IgG Alexa Fluor 488 (Invitrogen; A11029) antibody for 30 minutes. Cells were washed and stained with Hoechst (dilution 1:1,000, Invitrogen cat# H3570). Images were acquired with an Opera Phenix high content confocal microscope (PerkinElmer). The number of N- positive objects and nuclei were quantified using the Harmony software (PerkinElmer). The viral titer (Infectious units /mL) was calculated from the last positive dilution with 1 infectious unit (IU) being 3 times the background.

Antibodies

Bamlanivimab, Casirivimab, Etesevimab, Imdevimab, Cilgavimab, Tixagevimab and Sotrovimab were provided by CHR Orleans. Bebtelovimab was produced as previously described [47]. NCP-1 antibody was selected from a series of mouse monoclonal antibodies (mAbs) directed against recombinant SARS-CoV-2 nucleoprotein. Four BALB/c mice were immunized by intraperitoneal injections at 3-week intervals of 50 µg of recombinant SARS-CoV-2 nucleoprotein mixed with alum adjuvant. The two mice presenting the best immune response were selected and were given a daily intravenous booster injection of SARS-CoV-2 nucleoprotein for three days. Two days after the last boost, hybridomas were produced by fusing spleen cells with NS1 myeloma cells. The Hybridoma culture supernatants were screened for the presence of anti-SARS-CoV-2 nucleoprotein antibodies with an ELISA checking their capacity to bind nucleoprotein biotin conjugate. Selected hybridomas were subsequently cloned and antibodies were produced from culture supernatants and purified by protein A affinity chromatography.

Statistical analysis

Flow cytometry data were analysed using FlowJo v.10 (TriStar). Calculations were performed using Excel 365 (Microsoft). Figures were generated using Prism 9 (GraphPad Software). Statistical analysis was conducted using GraphPad Prism 9. Statistical significance between different groups was calculated using the tests indicated in each figure legend.

Data availability

All data supporting the findings of this study are available within the article or from the corresponding authors upon reasonable request without any restrictions.

References

1. Viana, R.*, et al.* Rapid epidemic expansion of the SARS-CoV-2 Omicron variant in southern Africa. *Nature* **603**, 679-686 (2022).
2. Tegally, H.*, et al.* Emergence of SARS-CoV-2 Omicron lineages BA.4 and BA.5 in South Africa. *Nature Medicine* **28**, 1785-1790 (2022).
3. Murray, C.J.L. COVID-19 will continue but the end of the pandemic is near. *The Lancet* **399**, 417-419 (2022).
4. Sun, K.*, et al.* SARS-CoV-2 transmission, persistence of immunity, and estimates of Omicron’s impact in South African population cohorts. *Science Translational Medicine* **14**, eabo7081 (2022).
5. Andrews, N.*, et al.* Covid-19 Vaccine Effectiveness against the Omicron (B.1.1.529) Variant. *New England Journal of Medicine* **386**, 1532-1546 (2022).
6. Abu-Raddad, L.J.*, et al.* Effect of mRNA Vaccine Boosters against SARS-CoV-2 Omicron Infection in Qatar. *New England Journal of Medicine* **386**, 1804-1816 (2022).
7. Kuhlmann, C.*, et al.* Breakthrough infections with SARS-CoV-2 omicron despite mRNA vaccine booster dose. *The Lancet* **399**, 625-626 (2022).
8. Walls, A.C.*, et al.* SARS-CoV-2 breakthrough infections elicit potent, broad and durable neutralizing antibody responses. *Cell* (2022).
9. Cele, S.*, et al.* Omicron extensively but incompletely escapes Pfizer BNT162b2 neutralization. *Nature* (2021).
10. Carreño, J.M.*, et al.* Activity of convalescent and vaccine serum against SARS-CoV-2 Omicron. *Nature* (2021).
11. Planas, D.*, et al.* Considerable escape of SARS-CoV-2 Omicron to antibody neutralization. *Nature* **602**, 671-675 (2022).
12. Cao, Y.*, et al.* BA.2.12.1, BA.4 and BA.5 escape antibodies elicited by Omicron infection. *Nature* **608**, 593-602 (2022).
13. Hachmann, N.P.*, et al.* Neutralization Escape by SARS-CoV-2 Omicron Subvariants BA.2.12.1, BA.4, and BA.5. *New England Journal of Medicine* **387**, 86-88 (2022).
14. Cao, Y.*, et al.* BA.2.12.1, BA.4 and BA.5 escape antibodies elicited by Omicron infection. *Nature* (2022).
15. Tuekprakhon, A.*, et al.* Antibody escape of SARS-CoV-2 Omicron BA.4 and BA.5 from vaccine and BA.1 serum. *Cell* **185**, 2422-2433.e2413 (2022).
16. Planas, D.*, et al.* Duration of BA.5 neutralization in sera and nasal swabs from SARS-CoV-2 vaccinated individuals, with or without omicron breakthrough infection. *Med* (2022).
17. Kurhade, C.*, et al.* Low neutralization of SARS-CoV-2 Omicron BA.2.75.2, BQ.1.1, and XBB.1 by 4 doses of parental mRNA vaccine or a BA.5-bivalent booster. *Biorxiv*, 2022.2010.2031.514580 (2022).
18. Qu, P.*, et al.* Distinct Neutralizing Antibody Escape of SARS-CoV-2 Omicron Subvariants BQ.1, BQ.1.1, BA.4.6, BF.7 and BA.2.75.2. *Biorxiv*, 2022.2010.2019.512891 (2022).
19. Sheward, D.J.*, et al.* Omicron sublineage BA.2.75.2 exhibits extensive escape from neutralising antibodies. *Biorxiv*, 2022.2009.2016.508299 (2022).
20. Wang, Q.*, et al.* Resistance of SARS-CoV-2 omicron subvariant BA.4.6 to antibody neutralisation. *The Lancet Infectious Diseases* (2022).
21. Hachmann, N.P., Miller, J., Collier, A.-r.Y. & Barouch, D.H. Neutralization Escape by SARS-CoV-2 Omicron Subvariant BA.4.6. *New England Journal of Medicine* (2022).
22. Miller, J.*, et al.* Substantial Neutralization Escape by the SARS-CoV-2 Omicron Variant BQ.1.1. *Biorxiv*, 2022.2011.2001.514722 (2022).
23. Cao, Y.*, et al.* Imprinted SARS-CoV-2 humoral immunity induces converging Omicron RBD evolution. *Biorxiv*, 2022.2009.2015.507787 (2022).
24. Park, Y.-J.*, et al.* Imprinted antibody responses against SARS-CoV-2 Omicron sublineages. *Science* **0**, eadc9127 (2022).

25. Collier, A.-r.Y.*, et al.* Immunogenicity of the BA.5 Bivalent mRNA Vaccine Boosters. *Biorxiv*, 2022.2010.2024.513619 (2022).

26. Davis-Gardner, M.E.*, et al.* mRNA bivalent booster enhances neutralization against BA.2.75.2 and BQ.1.1. *Biorxiv*, 2022.2010.2031.514636 (2022).

27. Wang, Q.*, et al.* Antibody responses to Omicron BA.4/BA.5 bivalent mRNA vaccine booster shot. *Biorxiv*, 2022.2010.2022.513349 (2022).

28. Osada, N.*, et al.* The genome landscape of the african green monkey kidney-derived vero cell line. *DNA Res* **21**, 673-683 (2014).

29. Ogando, N.S.*, et al.* SARS-coronavirus-2 replication in Vero E6 cells: replication kinetics, rapid adaptation and cytopathology. *Journal of General Virology* **101**, 925-940 (2020).

30. Meng, B.*, et al.* Altered TMPRSS2 usage by SARS-CoV-2 Omicron impacts infectivity and fusogenicity. *Nature* **603**, 706-714 (2022).

31. Cao, Y.*, et al.* Characterization of the enhanced infectivity and antibody evasion of Omicron BA.2.75. *Cell Host & Microbe* **30**, 1527-1539.e1525 (2022).

32. Puhach, O.*, et al.* Infectious viral load in unvaccinated and vaccinated individuals infected with ancestral, Delta or Omicron SARS-CoV-2. *Nature Medicine* **28**, 1491-1500 (2022).

33. Bénard, J.*, et al.* Characterization of a human ovarian adenocarcinoma line, IGROV1, in tissue culture and in nude mice. *Cancer Res* **45**, 4970-4979 (1985).

34. Buchrieser, J.*, et al.* Syncytia formation by SARS-CoV-2-infected cells. *EMBO J* **39**, e106267 (2020).

35. Planas, D.*, et al.* Sensitivity of infectious SARS-CoV-2 B.1.1.7 and B.1.351 variants to neutralizing antibodies. *Nature Medicine* (2021).

36. Gruell, H.*, et al.* Antibody-mediated neutralization of SARS-CoV-2. *Immunity* **55**, 925-944 (2022).

37. Taylor, P.C.*, et al.* Neutralizing monoclonal antibodies for treatment of COVID-19. *Nature Reviews Immunology* (2021).

38. O'Brien, M.P.*, et al.* Subcutaneous REGEN-COV Antibody Combination to Prevent Covid-19. *New England Journal of Medicine* **385**, 1184-1195 (2021).

39. Levin, M.J.*, et al.* Intramuscular AZD7442 (Tixagevimab–Cilgavimab) for Prevention of Covid-19. *New England Journal of Medicine* **386**, 2188-2200 (2022).

40. Gupta, A.*, et al.* Early Treatment for Covid-19 with SARS-CoV-2 Neutralizing Antibody Sotrovimab. *New England Journal of Medicine* **385**, 1941-1950 (2021).

41. WHO. Therapeutics and COVID-19: living guideline. Sept 16, 2022 Update *https://www.who.int/publications/i/item/WHO-2019-nCoV- therapeutics-2022.5* (2022).

42. NIH. COVID-19 treatment guidelines. *https://www.covid19treatmentguidelines.nih.gov/therapies/anti-sars-cov-2-antibody-products/* (2022).

43. Westendorf, K.*, et al.* LY-CoV1404 (bebtelovimab) potently neutralizes SARS-CoV-2 variants. *Cell Reports* **39**, 110812 (2022).

44. Hentzien, M., Autran, B., Piroth, L., Yazdanpanah, Y. & Calmy, A. A monoclonal antibody stands out against omicron subvariants: a call to action for a wider access to bebtelovimab. *The Lancet Infectious Diseases* **22**, 1278 (2022).

45. France, S.p. Point épidémiologique COVID-19 du 10 février 2022. . *https://www.santepubliquefrance.fr/presse/2022/point-epidemiologique-covid-19-du-10-fevrier-2022-le-ralentissement-de-la-circulation-du-sars-cov-2-se-confirme-et-s-accompagne-d-une-baisse-des* (2022).

46. Suzuki, R.*, et al.* Attenuated fusogenicity and pathogenicity of SARS-CoV-2 Omicron variant. *Nature* **603**, 700-705 (2022).

47. Bruel, T.*, et al.* Serum neutralization of SARS-CoV-2 Omicron sublineages BA.1 and BA.2 in patients receiving monoclonal antibodies. *Nature Medicine* **28**, 1297-1302 (2022).

48. Kimura, I.*, et al.* Virological characteristics of the SARS-CoV-2 Omicron BA.2 subvariants, including BA.4 and BA.5. *Cell* **185**, 3992-4007.e3916 (2022).

49.   Saito, A*., et al.* Virological characteristics of the SARS-CoV-2 Omicron BA.2.75 variant. *Cell Host & Microbe* **30**, 1540-1555.e1515 (2022).

50.   Arora, P*., et al.* Lung cell entry, cell-cell fusion capacity, and neutralisation sensitivity of omicron sublineage BA.2.75. *The Lancet Infectious Diseases* **22**, 1537-1538 (2022).

51.   Lee, W.S., Wheatley, A.K., Kent, S.J. & DeKosky, B.J. Antibody-dependent enhancement and SARS-CoV-2 vaccines and therapies. *Nature Microbiology* **5**, 1185-1191 (2020).

52.   Bruel, T*., et al.* Longitudinal analysis of serum neutralization of SARS-CoV-2 Omicron BA.2, BA.4 and BA.5 in patients receiving monoclonal antibodies. *medRxiv*, 2022.2008.2012.22278699 (2022).

53.   Martin-Blondel, G*., et al.* Sotrovimab to prevent severe COVID-19 in high-risk patients infected with Omicron BA.2. *J Infection* **85**, e104-e108 (2022).

54.   Wu, M.Y*., et al.* WHO's Therapeutics and COVID-19 Living Guideline on mAbs needs to be reassessed. *The Lancet* (2022).

55.   Park, Y.-J*., et al.* Imprinted antibody responses against SARS-CoV-2 Omicron sublineages. *Science* **378**, 619-627 (2022).

56.   Scheaffer, S.M*., et al.* Bivalent SARS-CoV-2 mRNA vaccines increase breadth of neutralization and protect against the BA.5 Omicron variant in mice. *Nature Medicine* (2022).

57.   Chalkias, S*., et al.* Safety, immunogenicity and antibody persistence of a bivalent Beta-containing booster vaccine against COVID-19: a phase 2/3 trial. *Nature Medicine* (2022).

58.   Cao, L*., et al.* Rapid evaluation of COVID-19 vaccine effectiveness against symptomatic infection with SARS-CoV-2 variants by analysis of genetic distance. *Nature Medicine* **28**, 1715-1722 (2022).

59.   Reynolds, C.J*., et al.* Immune boosting by B.1.1.529 (Omicron) depends on previous SARS-CoV-2 exposure. *Science* **377**, eabq1841 (2022).

60.   McCallum, M*., et al.* N-terminal domain antigenic mapping reveals a site of vulnerability for SARS-CoV-2. *Cell* **184**, 2332-2347.e2316 (2021).

61.   Ng, K.W*., et al.* SARS-CoV-2 S2–targeted vaccination elicits broadly neutralizing antibodies. *Science Translational Medicine* **14**, eabn3715 (2022).

62.   Buckner, C.M*., et al.* Interval between prior SARS-CoV-2 infection and booster vaccination impacts magnitude and quality of antibody and B cell responses. *Cell* **185**, 4333-4346.e4314 (2022).

63.   Monel, B*., et al.* Release of infectious virus and cytokines in nasopharyngeal swabs from individuals infected with non-alpha or alpha SARS-CoV-2 variants: an observational retrospective study. *eBioMedicine* **73**(2021).
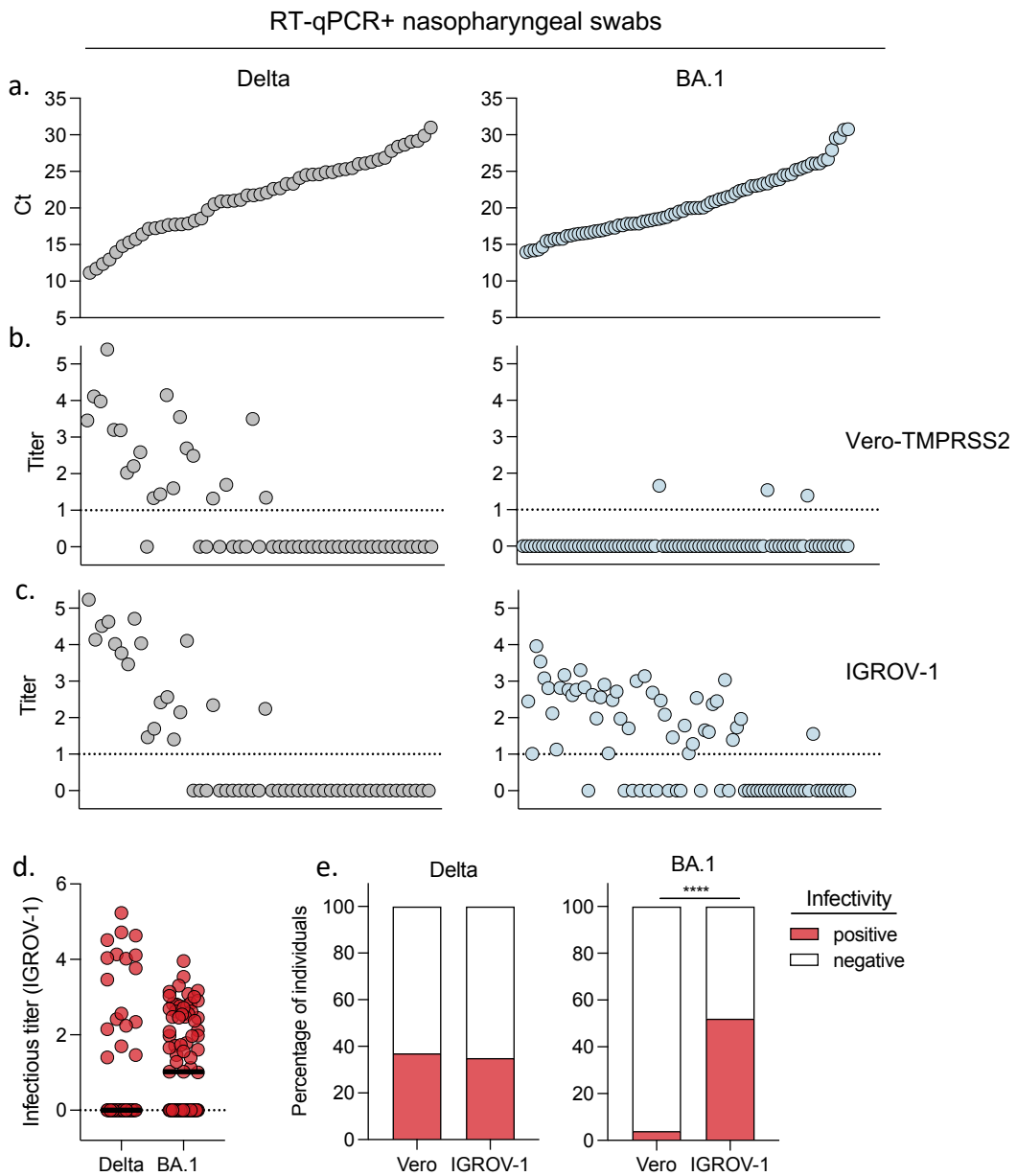
Figure 1. Improved detection of infectious Omicron BA.1 in nasopharyngeal swabs using IGROV-1 cells. A retrospective series of 135 RT+qPCR+ nasopharyngeal swabs from COVID-19 patients, harboring Delta (n=53) or Omicron BA.1 (n=82) variants was collected. **a.** Viral RNA loads, measured by RT-qPCR. The samples were ranked from high to low viral RNA load (low to high Ct). **b,c.** Viral titers were measured in Vero-TMPRSS2 (b) and IGROV-1 cells (c). Delta and Omicron BA.1-positive samples are depicted in the left and right panels, respectively. **d.** Comparison of infectious titers for Delta and BA.1 samples in IGROV-1 cells (left panel). Black lines represent the median values. **e.** Percentage of samples harboring detectable infectious Delta (middle panel) or BA.1 virus (right panel) using Vero and IGROV-1 cells. A Chi-square test was performed ****p<0.0001.
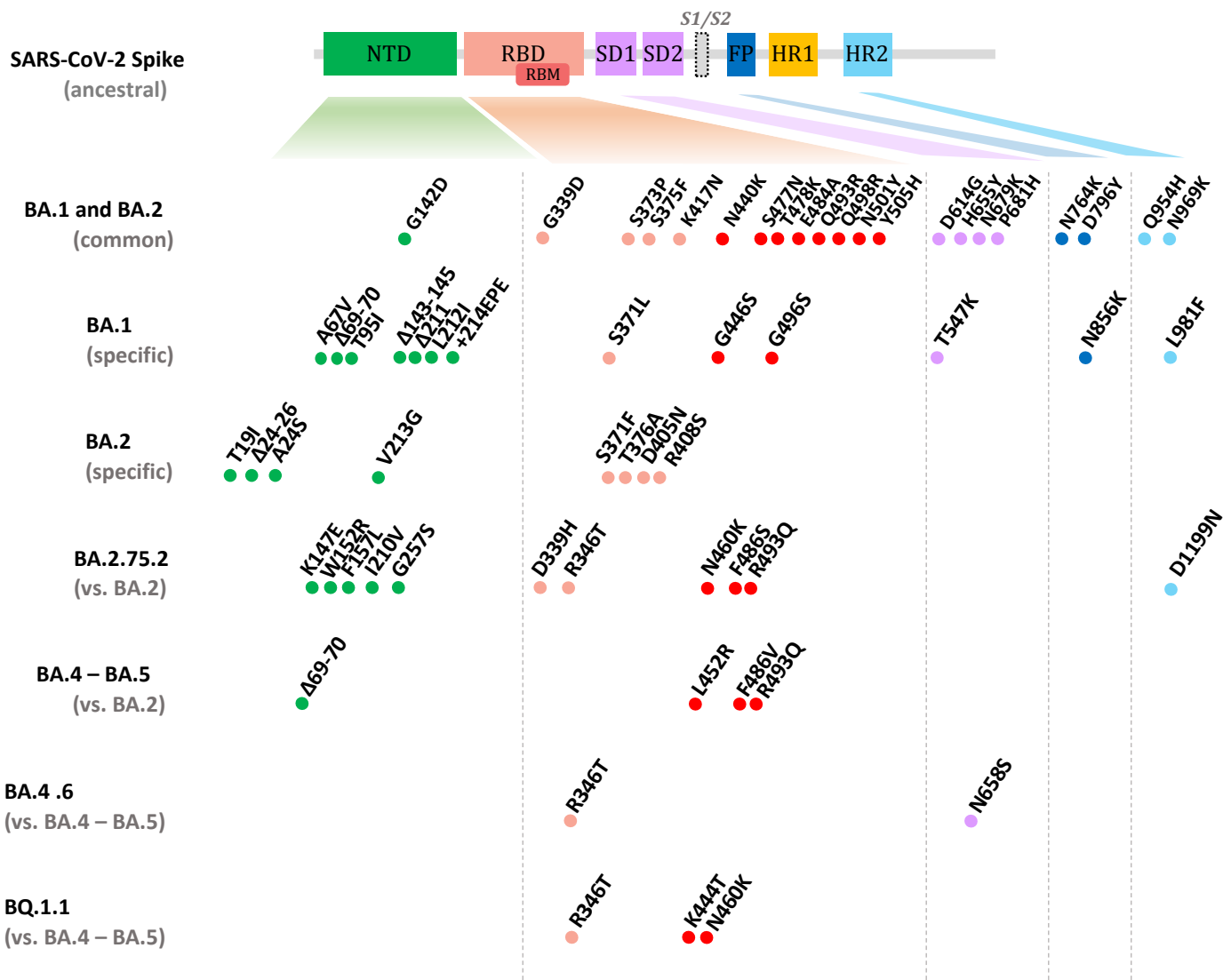
Figure 1

Figure 2. Mutations present in the spike proteins of Omicron subvariants. NTD, N-terminal domain; RBD, receptor binding domain; RBM, receptor binding motif; SD1, subdomain 1; SD2, subdomain 2; FP, fusion peptide; HR1, heptad repeat 1; HR2, heptad repeat 2. The BA.1 and BA.2 mutations are relative to the ancestral Wuhan sequence, the BA.2.75.2 mutations are relative to BA.2, the BA.4.6 and BQ.1.1 relative to BA.4/BA.5. Data are adapted from [22].

Figure 2

a.

● Delta ● BA.2.75.2 ● BA.4.6 ● BQ.1.1   Concentration (ng/mL)

b.

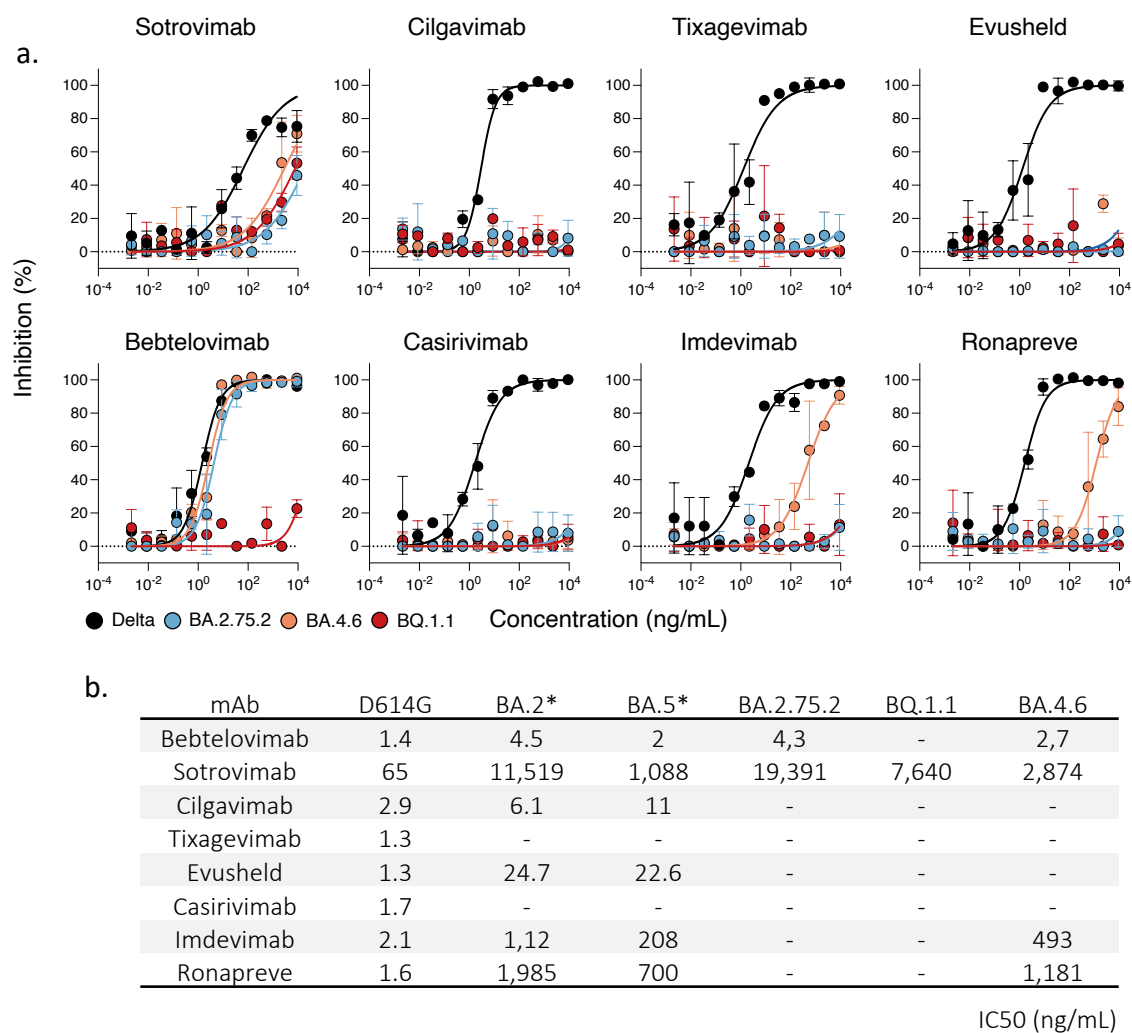| mAb	D614G	BA.2*	BA.5*	BA.2.75.2	BQ.1.1	BA.4.6
Bebtelovimab	1.4	4.5	2	4,3	-	2,7
Sotrovimab	65	11,519	1,088	19,391	7,640	2,874
Cilgavimab	2.9	6.1	11	-	-	-
Tixagevimab	1.3	-	-	-	-	-
Evusheld	1.3	24.7	22.6	-	-	-
Casirivimab	1.7	-	-	-	-	-
Imdevimab	2.1	1,12	208	-	-	493
Ronapreve	1.6	1,985	700	-	-	1,181

IC50 (ng/mL)

Figure 3. Neutralization activity of therapeutic monoclonal antibodies against BQ.1.1, BA.2.75.2 and BA.4.6. a. Neutralization curves of monoclonal antibodies. Dose–response analysis of the neutralization by the indicated antibodies or their clinical combinations. Evusheld: Cilgavimab and Tixagevimab. Ronapreve: Casirivimab and Imdevimab. Data are mean ± s.d. of 2 independent experiments. **b**. IC50 values in ng/ mL for each antibody against the indicated viral strains. *ED50 against BA.2 and BA.5 are from [47].
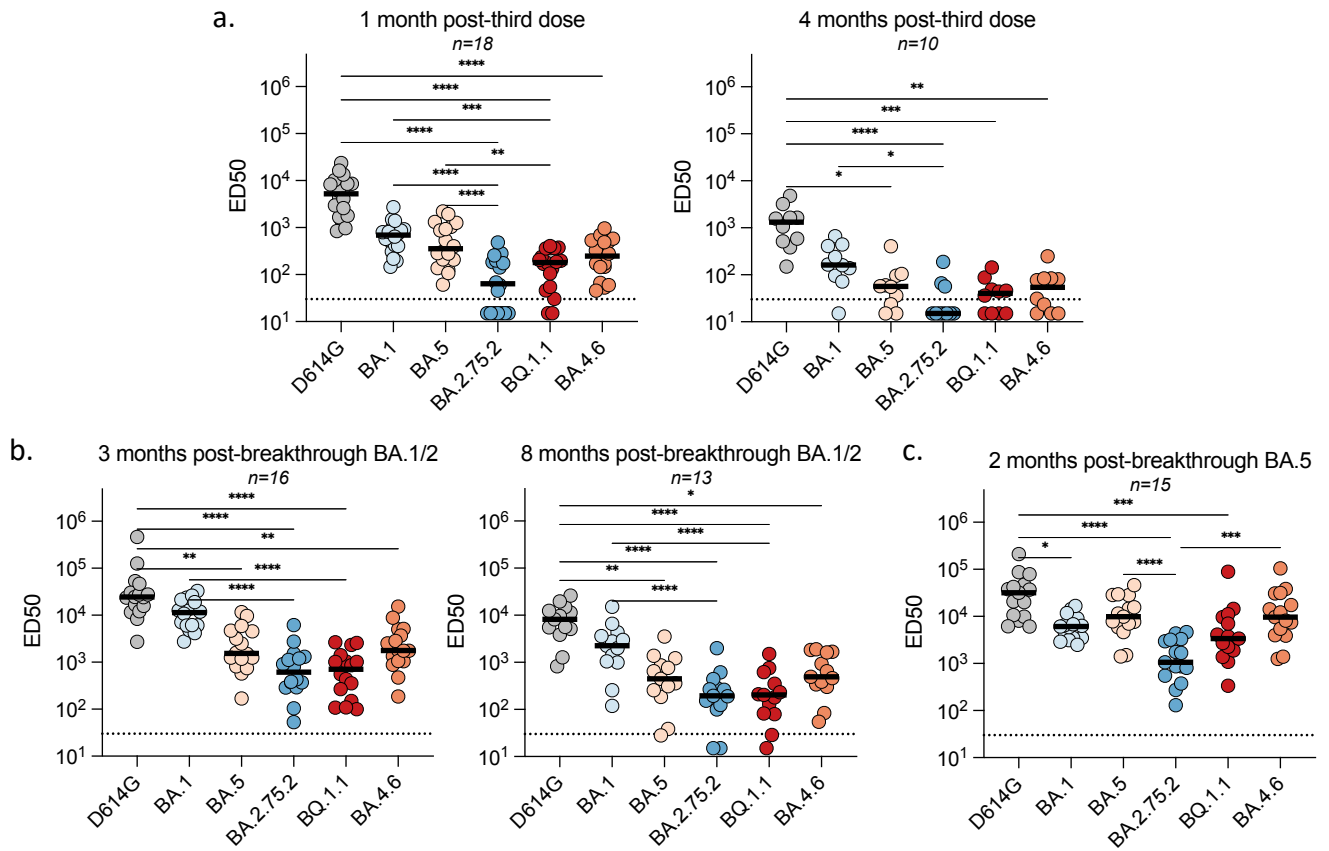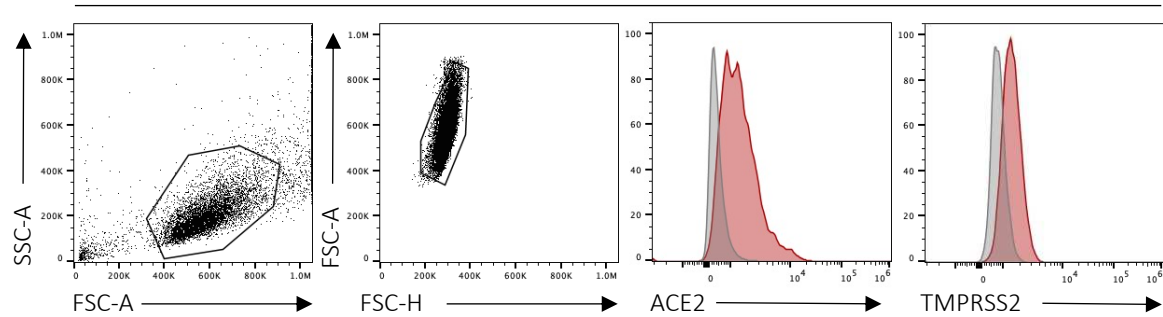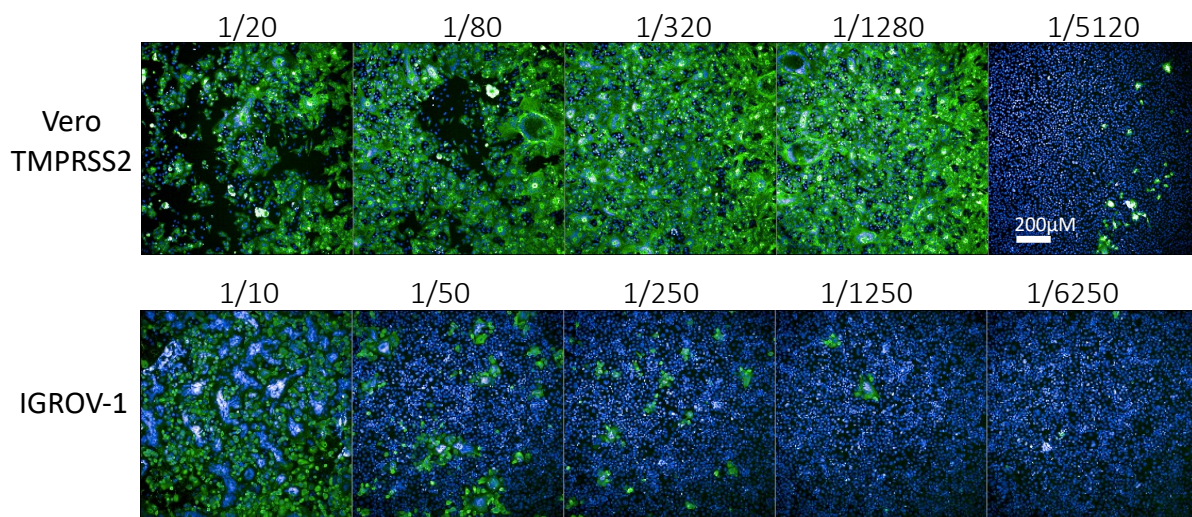
Figure 3

Figure 4. Sensitivity of SARS-CoV-2 D614G and Omicron subvariants to sera from vaccinated, or infected-then-vaccinated individuals. Neutralization titers of the sera against the indicated viral variants are expressed as ED50. **a,b.** Neutralizing activity of sera from individuals vaccinated with 3 doses of Pfizer vaccine. Sera were sampled at 1 month (a; n=18) and 4 months (b; n=10) after the third dose. **c,d.** Neutralizing activity of sera from Pfizer-vaccinated recipients after BA.1/BA.2 breakthrough infection. Sera were sampled about 3 months (c; n=16) and 8 months (d; n=13) after the breakthrough. **d.** Neutralizing activity of sera from Pfizer-vaccinated recipients after BA.5 breakthrough infection. Sera were sampled about 2 months after the breakthrough (n=15). The dotted line indicates the limit of detection (ED50 = 30). Black lines represent the median values. Two-sided Friedman test with Dunn's test for multiple comparisons was performed between each viral strain at the different time points; *p < 0.05; **p<0.001; ***p<0.0001; ****p < 0.0001.
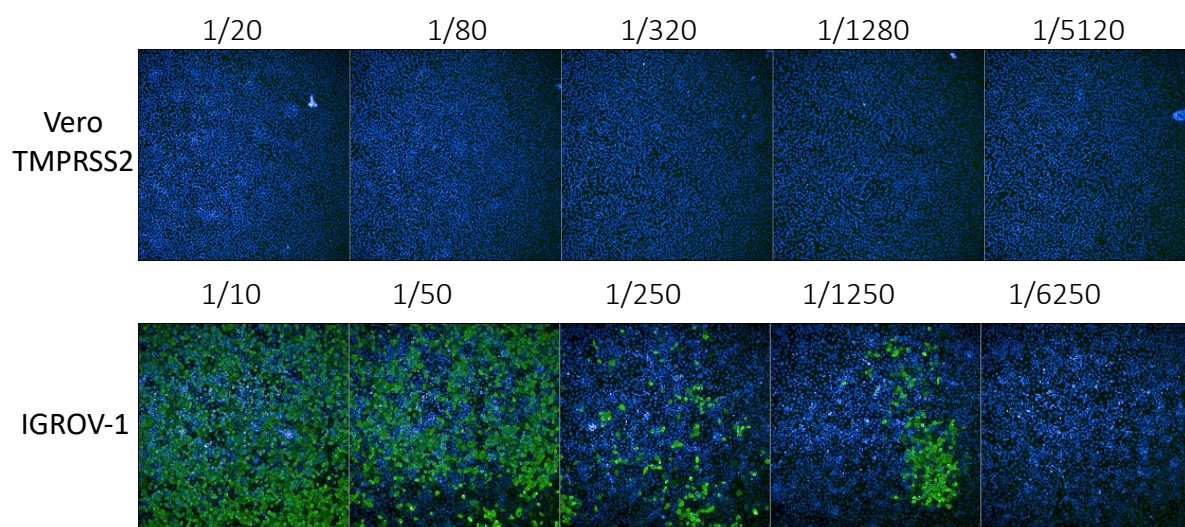
Figure 4

IGROV-1 cells

Extended data Figure 1. Phenotyping of IGROV-1 cells by flow cytometry. IGROV-1 cells were stained with anti-ACE2 and anti-TMPRSS2 antibodies and analyzed by flow cytometry. Representative examples of the gating strategy (left) and of the signals obtained are shown (right).
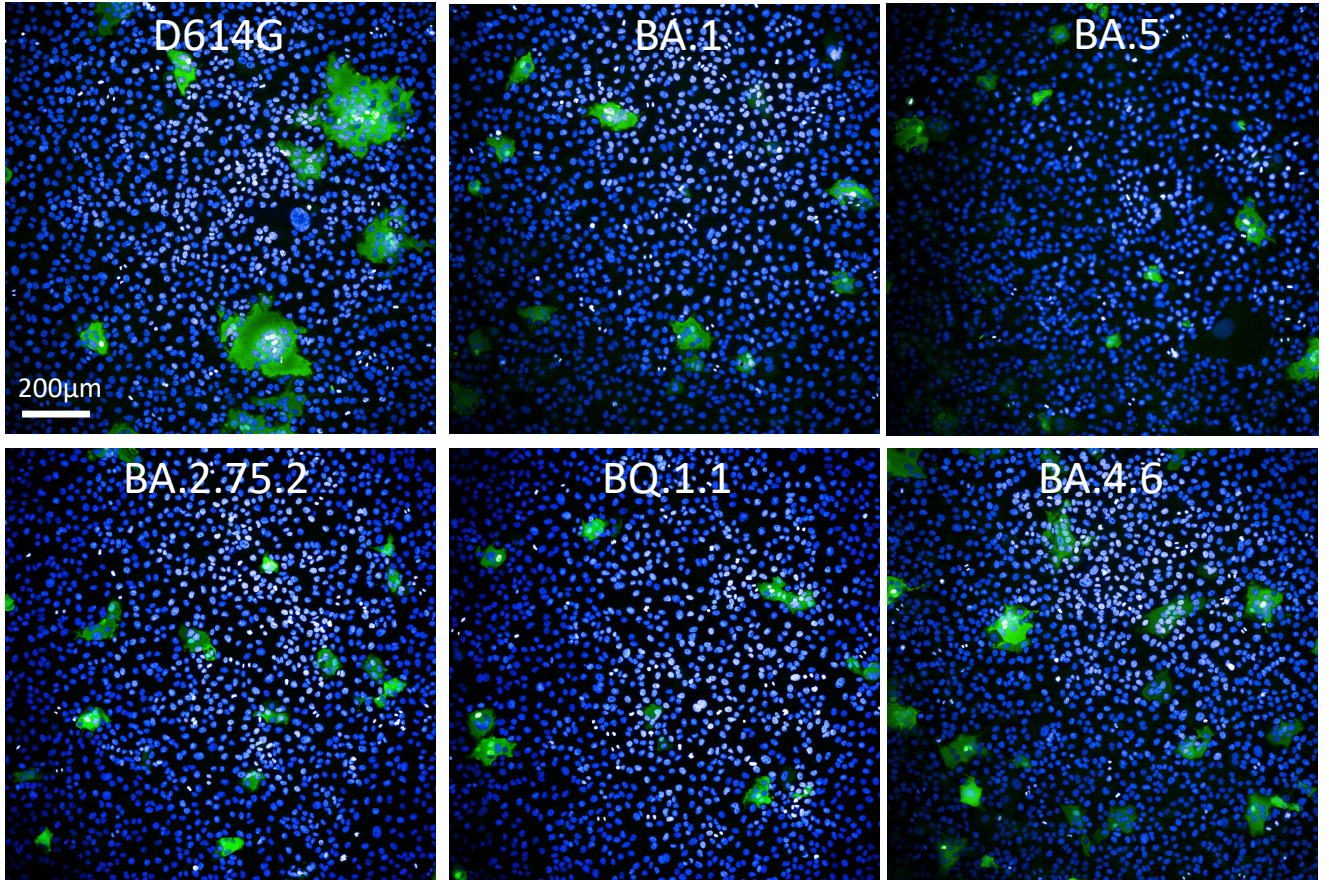
Delta+ nasopharyngeal swab

BA.1+ nasopharyngeal swab

Extended data Figure 2. Infectivity of Delta- and Omicron-positive nasopharyngeal swabs on Vero-TMPRSS2 and IGROV-1 cells. Nasopharyngeal swabs from either Delta or Omicron-infected individuals were cultivated on Vero-TMPRSS2 and IGROV-1 cells. Limiting dilution were performed to calculate viral infectivity titers. After 48h of culture, cells were stained using a pan-coronavirus anti-N antibody to visualize infection (AlexaFluor488 in green) and Hoechst to visualize nuclei (in blue). Both swabs have a RT-qPCR Cycle threshold (CT) of 16.4. Two representative individuals are displayed. Scale bar, 200 µm.

Extended data Figure 3. SARS-CoV-2 variants Delta, BA.1, BA.5, BA.2.75.2, BQ.1.1 and BA.4.6 induce syncytia in S-Fuse cells. S-Fuse cells that become GFP + upon cell-cell fusion were exposed to the indicated SARS-CoV-2 strains. After 20 h, cells were stained with Hoechst to visualize nuclei. Syncytia (green) and nuclei (blue) are shown. Representative images from three independent experiments are shown. Scale bar, 200 µm.

Delta positive nasopharyngeal swabs		
Sex	Female	25
	Male	28
Age (Median; range)		61 (24;98)
Immunodeficiency		6
Vaccination statut (Number of patients)		
	Unvaccinated	33
	1st dose	2
	2nd dose	10
	3rd dose	7
	4th dose	0
Sampling days post-symptom (median; range)		7 (0;30)

BA.1 positive nasopharyngeal swabs		
Sex	Female	49
	Male	32
Age (Median; range)		41 (19;98)
Immunodeficiency		7
Vaccination statut (Number of patients)		
	Unvaccinated	12
	1st dose	6
	2nd dose	41
	3rd dose	13
	4th dose	1
Sampling days post-symptom (median; range)		2 (0;21)

Supplemental table 1

1 month post-third dose

Sex	Female	8
	Male	10
Age (Median; range)		60 (36;95)
Immunodeficiency		0
Previous COVID-19		0
1st dose		Jan 6 - April 19, 2021
2nd dose		Jan 26 - May 31, 2021
3rd dose		Aug 31 - Dec 10, 2021
Sampling days post-vaccination (median; range)		34 days (24;54)

4 months post-third dose

Sex	Female	3
	Male	7
Age (Median; range)		63 (53;94)
Immunodeficiency		0
Previous COVID-19		0
1st dose		Jan 8 - Feb 4, 2021
2nd dose		Jan 29 - March 3, 2021
3rd dose		Sept 6 - Nov 16, 2021
Sampling days post-vaccination (median; range)		132 days (99;232)

3 months post-breakthrough BA.1/2

Sex	Female	7
	Male	9
Age (Median; range)		58 (34;72)
Immunodeficiency		0
Vaccination statut (Number of patients)		
3 doses		16
Breakthrough BA.1		Dec 26, 2021 - Jun 22, 2022
Sampling days post-breakthrough (median; range)		84 days (44;109)

8 months post-breakthrough BA.1/2

Sex	Female	5
	Male	8
Age (Median; range)		59 (36;72)
Immunodeficiency		0
Vaccination statut (Number of patients)		
3 doses		13
Breakthrough BA.1/BA.2		Dec 26, 2021 - April 14, 2022
Sampling days post-breakthrough (median; range)		234 days (142;289)

2 months post-breakthrough BA.5

Sex	Female	10
	Male	5
Age (Median; range)		62 (22;93)
Immunodeficiency		0
Vaccination statut (Number of patients)		
2 doses		1
3 doses		10
4 doses		4
Breakthrough BA.5 (days of positive PCR)		July 7 - Oct 10, 2022
Sampling days post-breakthrough (median; range)		50 days (12;127)